Mongolian Journal of Engineering and Applied Sciences, 2025, 7(1)
https://doi.org/10.22353/mjeas.v7i1.9635

Article

Synergistic antibacterial activity of ciprofloxacin-loaded silver and mesoporous silica core/shell nanoparticles

Jargalmaa Lunee[1], Nomin Tserendulam[2], Erdene Norov[1,*]

[1]Department of Chemical and Biological Engineering, School of Engineering and Technology, National University of Mongolia, Ulaanbaatar, Mongolia
[2]Department of Physics, Polytechnic University of Catalunya, Barcelona, Spain

Received on 2025.04.17; Revised on 2025.05.21; Accepted on 2025.05.27

*Corresponding author: erdene@num.edu.mn
ORCID:0000-0002-1775-068X

Abstract
The misuse and overuse of antibiotics have led to the rise of antibiotic-resistant microorganisms, which are projected to cause approximately 10 million deaths annually by 2050—surpassing cancer-related mortality. This growing crisis requires the development of new antibacterial strategies. Nanoparticles (NPs) have emerged as promising antimicrobial agents, with silver nanoparticles (AgNPs) demonstrating potent antibacterial activity through mechanisms such as controlled silver ion release, increased bacterial membrane permeability, and reactive oxygen species (ROS) generation. In this study, ciprofloxacin-loaded silver and mesoporous silica core/shell nanoparticles (CIPRO-Ag@MSNs) exhibited synergistic antibacterial effects against both Gram-positive bacteria (*Staphylococcus aureus* and *Micrococcus luteus*) and Gram-negative bacteria (*Escherichia coli* and *Pseudomonas aeruginosa*), significantly improving the efficacy of ciprofloxacin. Notably, mesoporous silica-coated silver nanoparticles (Ag@MSNs) improved biocompatibility by reducing excessive bacterial killing, highlighting their potential as a safe and effective nanosystem for bacterial infection treatment.

Key words: Ag@MSNs, ciprofloxacin, synergistic effect against bacteria

1 Introduction

A total of 97 antibiotics from eight different classes are used worldwide to treat bacterial infections. The global consumption of antibiotics has risen dramatically, reaching 40.2 billion defined daily doses in 2018—a 46% since 2000 [1]. However, the inefficacy of pathogen clearance and the rise of antimicrobial resistance have led to the emergence of multidrug-resistant (MDR) bacteria, posing severe threats to global health, potentially triggering a new pandemic, increasing the number of bacterial infection-related deaths, and underscoring the urgent need for novel antibiotic therapies.

Silver-based materials are highly active against pathogenic microorganisms such as bacteria, viruses, and fungi and have been widely used for therapeutic purposes since ancient times. Nano-sized silver particles exhibit a higher surface area to volume ratio than bulk silver, providing a larger surface for interaction with microorganisms and enhancing antimicrobial activity. In addition, the shape, size, surface area, morphology, surface charge, and physicochemical properties of the nanoparticles influence their antibacterial activity through various mechanisms [2]. Silver nanoparticles exert antibacterial effects by accumulating on the surface of bacterial cells, damaging the morphological structure of the cell wall and membrane, penetrating the cytoplasm, disrupting the function of cellular organelles, releasing free metal ions, generating reactive oxygen species (ROS), and damaging DNA. Silver ions (Ag^+) also enter cells and interact with carbonyl, amine, phosphate, and thiol groups of cellular biomolecules such as DNA, proteins, and lipids. This interaction blocks the active site of enzymes that bind to substrates, leads to chromosomal DNA degradation, disrupting DNA replication, and inhibits protein synthesis, ultimately resulting in cell death [3, 4]. The effects of nanoparticles on Gram-positive and Gram-negative bacterial species differ due to variations in bacterial cell wall structure. Numerous studies have demonstrated that the antibacterial effect of nanoparticles is stronger against Gram-negative bacteria than Gram-positive bacteria. This difference is attributed to the structural characteristics of bacterial cell walls: Gram-positive bacteria have a thick, multilayered peptidoglycan layer, whereas Gram-negative bacteria have a thinner peptidoglycan layer and an additional outer membrane containing lipopolysaccharide (LPS) [5, 6].

Nanoparticle-antibiotic composites can mitigate bac-

terial antibiotic resistance and enhance antibiotic efficacy, thereby reducing both antibiotic toxicity and dosage requirements [7].

Nanoparticles exert antibacterial effects through multiple mechanisms, making it difficult for microorganisms to develop resistance. In other words, the probability of simultaneous mutations leading to resistance is extremely low. Furthermore, when nanoparticles are combined with antimicrobial drugs, the likelihood of resistance mutations occurring decreases even further [8].

A recent study by Yao Wang et al. demonstrated that levofloxacin-loaded, silver core-embedded mesoporous silica nanoparticles (Ag@MSNs@LEVO) exhibit synergistic antibacterial activity against drug-resistant bacteria. Notably, this nanosystem showed no toxic side effects in mice due to the protective mesoporous silica shell [9].

Mesoporous silica nanoparticles (MSNs) are well-known for their high surface area, tunable mesopores, ease of functionalization, and biocompatibility, making them prominent nanocarriers [10–14]. Silver-core and silica-shell mesoporous nanoparticles integrate an inner Ag core, which acts as a sustained silver ion source, with a mesoporous silica shell that serves as both a drug reservoir and a controlled release system. This single-particle nanoplatform enables the simultaneous release of antibiotics and Ag^+ ions, enhancing antibacterial efficacy [9, 15].

Ciprofloxacin, a quinolone antibiotic, is effective against both Gram-positive and Gram-negative bacteria and is widely used to treat various bacterial infections [16].

2 Materials and Methods

2.1 Materials

Silver nitrate ($AgNO_3$, 99.5 %), sodium borohydride ($NaBH_4$,AR), were purchased from Xilong Scientific Co., Ltd., China. Ethanol (CH_3CH_2OH, 99.9%), cetyltrimethylammonium bromide (CTAB, 99%), and tetraethyl orthosilicate (TEOS, 99 %) were obtained from Shanghai Macklin Biochemical Co., Ltd., China. Ciprofloxacin was purchased from the North China Pharmaceutical Group. Mueller-Hinton agar (MHA) medium was supplied by HiMedia Ltd.

2.2 Synthesis of silver and silica core/shell nanoparticles (Ag@MSNs)

Silver and silica core/shell nanoparticles (Ag@MSNs) were synthesized following the protocol described by Sandra-Montalvo Quiros et al. [7]. First, an aqueous solution of silver nitrate ($AgNO_3$, 0.1 M, 10 mL) was added to 40 mL of 0.1 M cetyltrimethylammonium bromide (CTAB) solution in an opaque flask maintained at 30–35°C to prevent the precipitation of silver bromide (AgBr). Then 10 mL of 0.2 M sodium borohydride ($NaBH_4$) was slowly added under vigorous stirring and allowed to react overnight in the dark. Next, 170 mL of 6 mM CTAB solution was mixed with 75 mL of ethanol under vigorous stirring at 35^oC. Once the temperature stabilized and the solution became clear and bubble-free, 100 µL of ammonia solution (NH_3, 25 vol%) was introduced. After 5 minutes, 5 mL of the freshly prepared silver nanoparticle solution was added to the mixture. Subsequently, 200 µL of tetraethyl orthosilicate (TEOS) was added dropwise to the reaction solution. The temperature was then raised to 55°C, and the reaction was stirred vigorously overnight in a dark environment. The resulting nanoparticles were collected by centrifugation at 14,000 rpm for 20 minutes and washed with ethanol. To remove the surfactant CTAB, the nanoparticles were dispersed in ethanol and sonicated in an ultrasonic bath for 2 hours. Finally, the purified nanoparticles were collected by centrifugation.

2.3 Loading ciprofloxacin into nano carriers

For drug loading, 20 mg of Ag@MSNs nanocarriers were mixed with a 5 mg/mL aqueous solution of ciprofloxacin and sonicated for 2 hours [9]. The ciprofloxacin-loaded Ag@MSNs were then collected by centrifugation at 10,000 rpm for 20 minutes.

2.4 Characterization

The synthesized materials were characterized using the following analytical techniques: UV-visible spectroscopy (Shimadzu UV-1650PC), Fourier transform infrared (FTIR) spectroscopy (Shimadzu IR Prestige), and scanning electron microscopy (SEM) (ZEISS SIGMA 500 VP). The hydrodynamic diameter distribution was determined using a Sympatec NANOPHOX NX0137. Nitrogen sorption isotherms were measured with an Autosorb-iQ, and the Brunauer-Emmett-Teller (BET) method was employed to determine specific surface areas based on data within a linear relative pressure range of 0.2–0.4. The pore size distribution was derived from the desorption branch of the isotherm using the Barrett-Joyner-Halenda (BJH) method. The total pore volume was determined via a single-point measurement of the adsorbed nitrogen amount at a relative pressure (P/P_0) of 0.99.

2.5 Disk diffusion test

Gram-positive bacteria (*Staphylococcus aureus* and *Micrococcus luteus*) and Gram-negative bacteria (*Escherichia coli* and *Pseudomonas aeruginosa*) were selected as model organisms. The bacteria were cultured in nutrient broth at 37°C for 18 hours until reaching an optical density (OD600). Subsequently, 0.2 mL of the

bacterial suspension was evenly spread onto Mueller-Hinton agar plates. Sterile disks were placed on the agar surface, and the test sample was applied to each disk. The plates were then incubated at 37°C for 24 hours. After incubation, the zone of inhibition was measured from edge to edge across the clear zone, passing through the center of the disk.

3 Results

3.1 Characterization of Ag@MSNs

Ag@MSNs were synthesized via a combination of reduction and sol-gel reactions. This facile and soft synthesis was performed in deionized water, utilizing silver nitrate ($AgNO_3$) as the silver precursor, sodium borohydride ($NaBH_4$) as the reducing agent, cetyltrimethylammonium bromide (CTAB) as the surfactant, tetraethyl orthosilicate (TEOS) as the silica shell precursor, and ammonium solution (NH_3) as a pH modifier. As shown in the SEM images, the synthesized Ag@MSNs exhibited a uniform, monodisperse, spherical morphology with an average particle size of 89 ± 14 nm. Each Ag@MSN contained a single silver core at its center, with an average core diameter of 18 ± 5 nm (Figure 1).

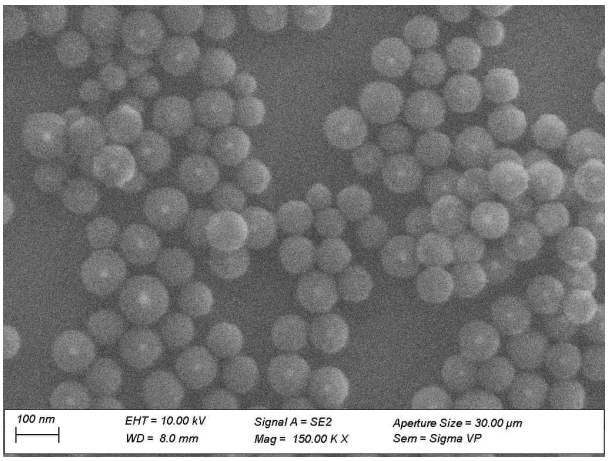

Figure 1: SEM image of Ag@MSNs.

The UV–Vis spectrometry results for AgNPs and Ag@MSNs core/shell nanoparticles are presented in Figure 2. As shown, the absorption spectrum of AgNPs exhibits a peak at 407 nm, corresponding to the plasmon resonance band of silver nanoparticles with a size smaller than 20 nm [8]. However, after coating with mesoporous silica, the absorption peak undergoes a red shift to 420 nm (red-shift), accompanied by a decrease in frequency and energy, as well as a 2.4-fold broadening of the full width at half maximum (FWHM). This shift is consistent with the well-established phenomenon that increasing the thickness of core/shell nanoparticles enhances absorption intensity and shifts the peak toward longer wavelengths [17]. The broadening of the absorption peak can be attributed to the quantum confinement effect, in which an increase in particle size leads to a reduction in band gap energy, thereby causing a red shift [18]. Figure 3 confirms the complete removal of CTAB molecules, as analyzed by infrared spectroscopy. If CTAB had not been fully eliminated, its characteristic bond vibrations would have been detected. Specifically, symmetric and asymmetric stretching vibrations of CH_2 bond would appear in the 2859 cm^{-1} and 2920 cm^{-1}.

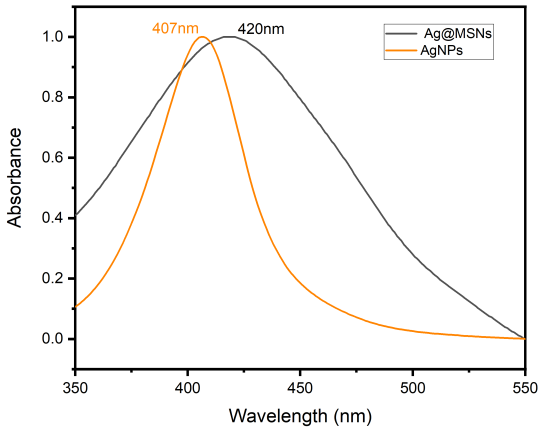

Figure 2: UV-vis absorption spectrum of Ag@MSNs and AgNPs in deionized water.

Additionally, the symmetric scissoring deformation of CH_3N^+ and CH_2, C-H bonds would be observed at 1419 cm^{-1}, 1486 cm^{-1}, and 1652 cm^{-1} [19–21]. The FTIR spectra of ciprofloxacin-loaded silver and silica core/shell nanoparticles (CIPRO-Ag@MSNs) are also shown in Figure 3. The peak at 3409 cm^{-1} corresponds to the carboxyl group of ciprofloxacin and the hydroxyl group of Ag@MSNs.

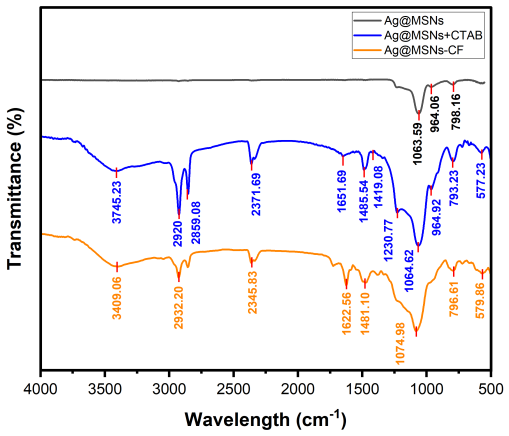

Figure 3: FTIR spectra of Ag@MSNs, Ag@MSNs with CTAB and ciprofloxacin loaded Ag@MSNs.

Ciprofloxacin exhibits characteristic peaks at 2932 cm^{-1}, 1481 cm^{-1}, and 1623 cm^{-1}, which correspond

to CH_2, C=CH, and Ar-H bond vibrations in the benzene ring. Additionally, the peak at 1075 cm^{-1} is attributed to both the C-F stretching vibration of ciprofloxacin and the Si-OH stretching vibration of Ag@MSNs. The peak at 797 cm^{-1} aligns with the Si-O-Si symmetric stretching bond vibrations, which are observed at 799 cm^{-1} and 815 cm^{-1} in Ag@MSNs and mesoporous silica nanoparticles. The peaks at 2346 cm^{-1} and 580 cm^{-1} correspond to the C=O bond and the Si-O-Si bending vibration of the carboxyl group of ciprofloxacin, respectively.

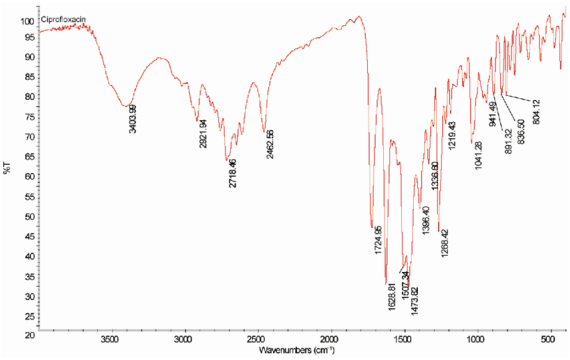

Figure 4: FTIR spectra of ciprofloxacin [22]

Those peaks may have undergone a spectral shift due to weak hydrogen interactions. Furthermore, the peak at 580 cm^{-1} may also be associated with the shifted peak of the quinoline ring in ciprofloxacin [22–26]. This result corresponds well with the FTIR findings (Figure 4) of ciprofloxacin antibiotic from the study conducted by Zhengde Tan et al [22].

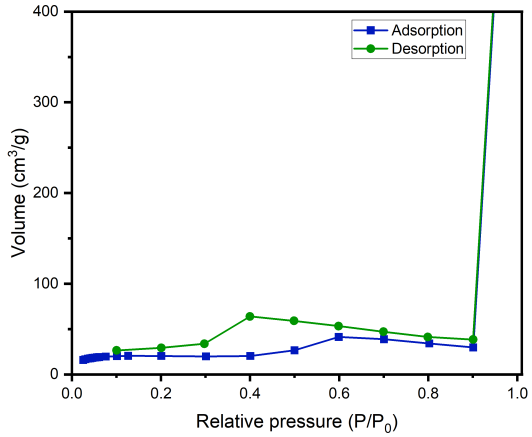

Figure 5: Nitrogen sorption isotherm curve of Ag@MSNs.

The pore characterization of Ag@MSNs was analyzed using N_2 sorption analysis (Figures 5 and 6). The adsorption-desorption isotherms exhibit a type IV Brunauer-Emmett-Teller (BET) isotherm with an H1-type hysteresis loop, indicating a uniform, cylindrical pore structure. The N_2 isotherms of Ag@MSNs show an inflection at a relative pressure of 0.2–0.4, which corresponds to the phenomenon of capillary condensation and evaporation [7]. The BET-specific surface area was determined to be 82 m^2/g at a relative pressure (P/P_0) of 0.99. According to the pore size distribution curve obtained by the Barrett-Joyner-Halenda (BJH) method, an intense peak is centered at a pore size of 5.5 nm with a pore volume of 1.23 cm^3/g. The results of the hydrodynamic size distribution of AgNPs and Ag@MSNs are shown in Figure 7. The measurements indicate that the silver nanoparticles have a size distribution ranging from 30 to 65 nm, with an average size of 47 nm. The hydrodynamic size, which represents the diameter of the nanoparticles in solution, is nearly twice as large as that observed in SEM images.

This discrepancy is attributed to the adsorption of solvent molecules onto the nanoparticle surface and the formation of a hydrate shell [19]. The particle size distribution of Ag@MSNs ranges from 200 to 375 nm, with an average size of 279 nm, indicating that the majority of the particles in solution fall within this size range [7].

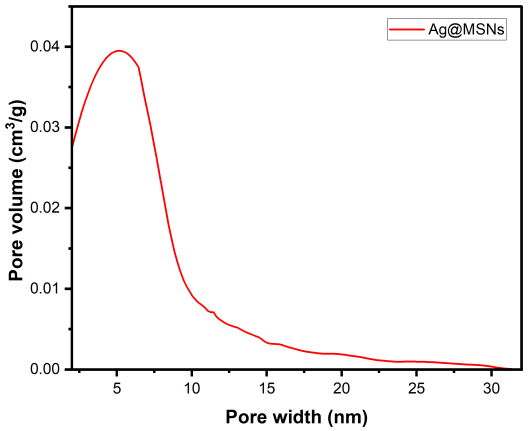

Figure 6: Pore size distribution of Ag@MSNs.

3.2 Antibacterial activity of CIPRO-Ag@MSNs

The antibacterial activity of CIPRO-Ag@MSNs against Gram-positive (*Staphylococcus aureus, Micrococcus luteus*) and Gram-negative (*Escherichia coli, Pseudomonas aeruginosa*) bacteria was evaluated using the disk diffusion method on MHA solid medium. The results are presented in Figures 8.

The study found that ciprofloxacin at a concentration of 0.1 μg/mL did not inhibit the growth of *S. aureus, M. luteus, E. coli,* or *P. aeruginosa.* However, at concentrations of 100 and 200 μg/mL, it produced excessively large inhibition zones. Therefore, the optimal concentrations of ciprofloxacin for bacterial inhibition were determined to be 10 and 50 μg/mL. Among the tested bacteria, ciprofloxacin exhibited the highest antibacterial activity against *E. coli* and the lowest activity against *M. luteus.* This variation is likely due to the

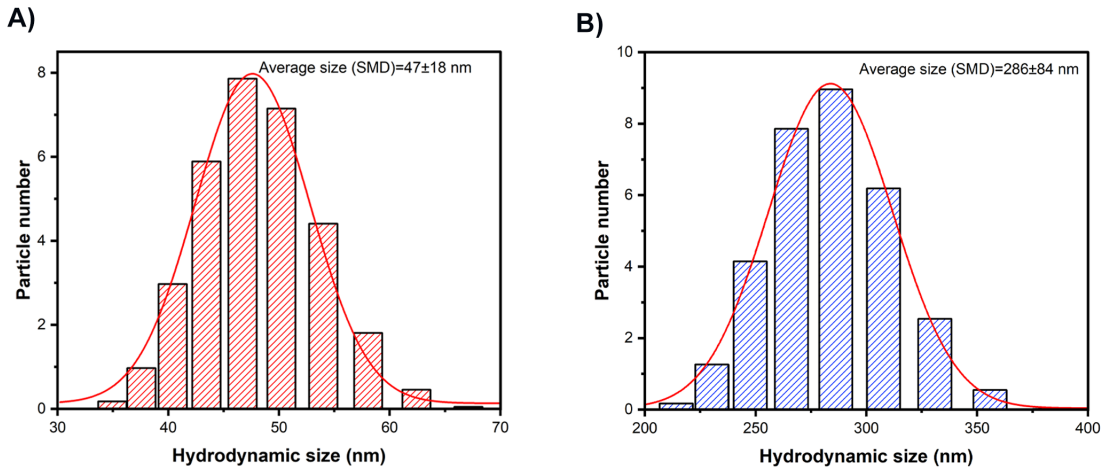

Figure 7: Hydrodynamic size distribution of A) AgNPs and B) Ag@MSNs in deionized water.

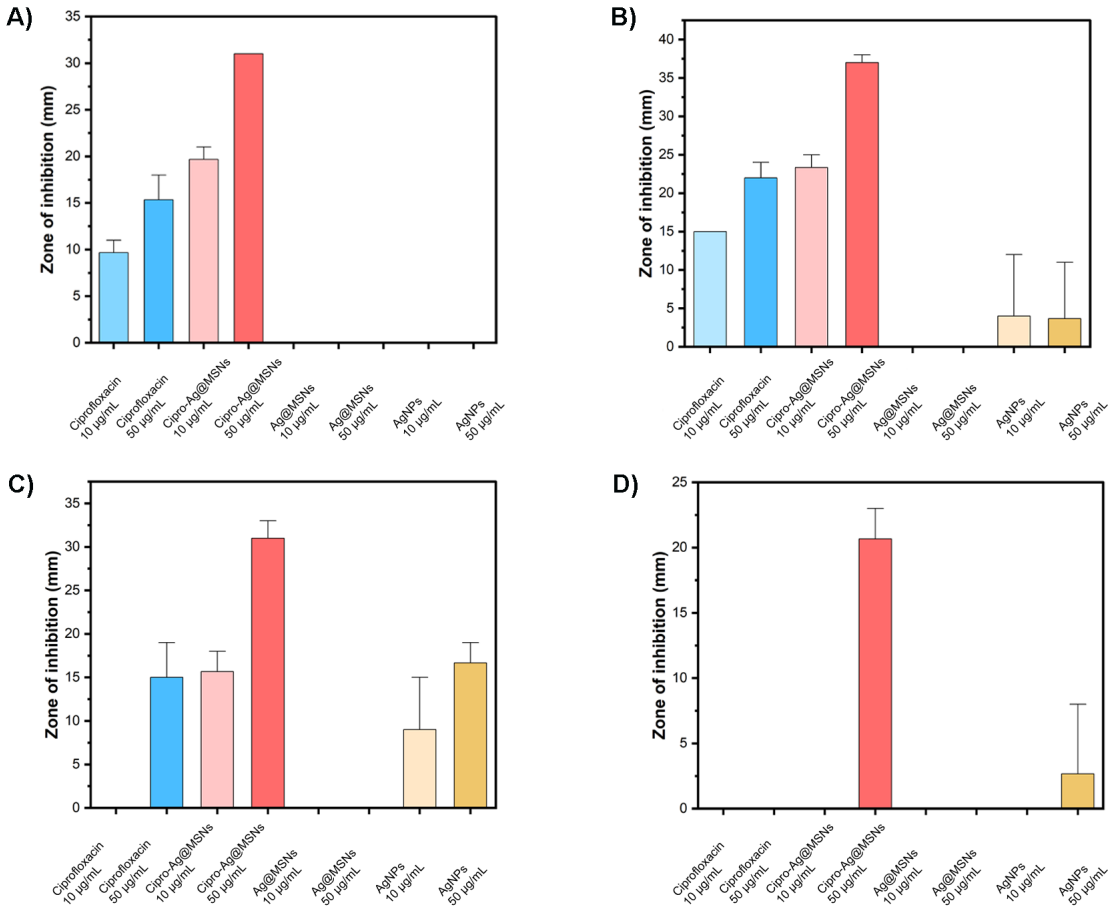

Figure 8: A) Antimicrobial inhibition zone in P. aeruginosa B) Antimicrobial inhibition zone in E. coli C) Antimicrobial inhibition zone in S.aurus D)Antimicrobial inhibition zone in M. luteus

thinner peptidoglycan layer in the cell wall of Gram-negative bacteria, which allows for better drug penetration. Despite these differences, ciprofloxacin effectively inhibited both Gram-positive and Gram-negative bacteria, demonstrating its broad spectrum antibacterial potential.

The optimal concentrations of silver nanoparticles (AgNPs) required to inhibit the growth of *S. aureus, M. luteus, E. coli*, and *P. aeruginosa* were determined to be 50 and 100 μg/mL. The antibacterial activity of AgNPs against Gram-positive bacteria (*S. aureus* and *M. Luteus*) was slightly higher than that of ciprofloxacin. However, their inhibitory effect on Gram-negative bacteria (*E. coli* and *P. Aeruginosa*) was approximately two times lower. This suggests that the antibacterial efficacy of AgNPs is influenced by their ability to penetrate the peptidoglycan layer of bacterial cell walls.

After coating the AgNPs with mesoporous silica, their antibacterial activity significantly decreased. In other words, Ag@MSNs alone were unable to effectively kill bacteria within the 20-hour experimental period. However, when ciprofloxacin was loaded onto Ag@MSNs, their antibacterial activity increased by 2- to 6-fold compared to ciprofloxacin alone. For instance, Ag@MSNs at a concentration of 10 μg/mL produced inhibition zones against *S. aureus* and *E. coli* comparable to those of ciprofloxacin at 50 μg/mL. This enhancement can be attributed to the synergistic effect between nanoparticles and ciprofloxacin, where Ag@MSNs are believed to facilitate bacterial cell damage and enhance drug penetration.

These findings are consistent with previous studies. Yao Wang et al. reported that silver/silica mesoporous core-shell nanoparticles loaded with levofloxacin at 40 μg/mL exhibited similar antibacterial activity against *E. coli* as levofloxacin alone at 300 μg/mL. Similarly, Duaaa R. Ibraheem et al. demonstrated that a combined system of silver nanoparticles and ciprofloxacin resulted in a two-fold increase in inhibition zone against *S. aureus* compared to either ciprofloxacin or AgNPs alone [9, 27].

4 Conclusions

In this work, we successfully synthesized silver and silica core-shell mesoporous nanoparticles (Ag@MSNs) with an average size of 89 nm and a pore diameter of 5.5 nm. Furthermore, we developed ciprofloxacin-loaded Ag@MSNs (CIPRO-Ag@MSNs), which exhibited a synergistic antibacterial effect against both Gram-positive and Gram-negative bacteria. Notably, Ag@MSNs alone exhibited no significant adverse effects on bacterial viability during the tested period, indicating their biocompatibility. However, when ciprofloxacin loaded, Ag@MSNs significantly enhanced antibacterial efficacy, suggesting their potential as an effective nanosystem for bacterial infection therapy.

Acknowledgements

The authors gratefully acknowledge the Nanomaterials Laboratory at the National University of Mongolia for their assistance with the synthesis and characterization of nanoparticles. Additionally, we extend our sincere appreciation to Associate Professor Radnaabazar Chinzorig and his team for their valuable support with the antibacterial activity test method.

Author Contributions

Norov Erdene: Conceptualization, project administration, review and editing, supervision. Jargalmaa Lunee: methodology, investigation, analysis, data curation, and writing the original draft. Nomin Tserendulam: investigation, methodology and data curation

Funding

This research was supported by the Science and Technology Foundation of Mongolia (Project №: ShUSs2018/59) and the Young Research Grant A/17.

Conflict of Interest

The authors declare no conflict of interest.

References

[1] Browne AJ, Chipeta MG, Haines-Woodhouse G, Kumaran EPA, Hamadani BHK, Zaraa S, et al. Global antibiotic consumption and usage in humans, 2000–18: a spatial modelling study. The Lancet Planetary Health. 2021;5:e893-904. doi:https://doi.org/10.1016/S2542-5196(21)00280-1.

[2] Baptista PV, McCusker MP, Carvalho A, Ferreira DA, Mohan NM, Martins M, et al. Nano-Strategies to fight multidrug resistant bacteria-"A battele of the titans". Frontiers in Microbiology. 2018 Jul;9:1441. doi:https://doi.org/10.3389/fmicb.2018.01441.

[3] Ozdal M, Gurkok S. A Recentadvances in nanoparticles as antibacterial agent. ADMET and DMPK. 2022. doi:https://doi.org/10.5599/admet.1172.

[4] Tang S, Zheng J. Antibacterial Activity of Silver Nanoparticles: Structural Effects. Advanced Healthcare Materials. 2018;7. doi:https://doi.org/10.1016/j.mset.2020.09.002.

[5] Tiwari S, Jamal SB, Hassan SS, Carvalho PVSD, Almeida S, Barh D, et al. Two-Component Signal Transduction Systems of Pathogenic Bacteria As Targets for Antimicrobial Therapy: An Overview. Frontiers in Microbiology. 2017;8:1878. doi:https://doi.org/10.3389/fmicb.2017.01878.

[6] Manzoor S, Bashir DJ, Imtiyaz K, Rizvi MMA, Ahamad I, Fatma T, et al. Biofabricated platinum nanoparticles: therapeutic evaluation as a potential nanodrug against breast cancer cells and drug-resistant bacteria. RSC Advances. 2021;11:24900-16. doi:https://doi.org/10.1039/D1RA03133C.

[7] Montalvo-Quirós S, Gómez-Graña S, Vallet-Regí M, Prados-Rosales RC, González B, Luque-Garcia JL. Mesoporous silica nanoparticles containing silver as novel antimycobacterial agents against Mycobacterium tuberculosis. Colloids and Surfaces B: Biointerfaces. 2021;197:111405. doi:https://doi.org/10.1016/j.colsurfb.2020.111405.

[8] Bastús NG, Merkoçi F, Piella J, Puntes V. Synthesis of Highly Monodisperse Citrate-Stabilized Silver Nanoparticles of up to 200 nm: Kinetic Control and Catalytic Properties. Chemistry of Materials. 2014;26:2836-46. doi:https://doi.org/10.1021/cm500316k.

[9] Wang Y, Ding X, Chen Y, Guo M, Zhang Y, Guo X, et al. Antibiotic-loaded, silver core-embedded mesoporous silica nanovehicles as a synergistic antibacterial agent for the treatment of drug-resistant infections. Biomaterials. 2016;101:207-16. doi:https://doi.org/10.1016/j.biomaterials.2016.06.004.

[10] M Vallet-Regi RPdR A Rámila, Pérez-Pariente J. A New Property of MCM-41:Drug Delivery System. Chem Mater. 2000 Dec:308-11. doi:https://doi.org/10.1021/cm0011559.

[11] María Vallet-Regí MM Montserrat ColiIsabel Izquierdo-Barba. Mesoporous Silica Nanoparticles for Drug Delivery: Current Insights. Molecules. 2008;23(1):47. doi:https://doi.org/10.3390/molecules23010047.

[12] Jonas G Croissant NMK Yevhen Fatieiev. Degradability and Clearance of Silicon, Organosilica, Silsesquioxane, Silica Mixed Oxide, and Mesoporous Silica Nanoparticles. Advanced Materials. 2017. doi:https://doi.org/10.1002/adma.201604634.

[13] Paris JL, Colilla M, Isabel Izquierdo-Barba MM, Vallet-Regí M. Tuning mesoporous silica dissolution in physiological environments: a review. Journal of Material science. 2017;52:61-71. doi:https://link.springer.com/article/10.1007

[14] María Vallet-Regí DA Francisco Balas. Mesoporous materials for drug delivery. Angew Chem Int Ed Engl. 2007;46(40):7548-58. doi:https://doi.org/10.1002/anie.200604488.

[15] Lu M, Wang Q, Chang Z, Wang Z, Zheng X, Shao D, et al. Synergistic bactericidal activity of chlorhexidine-loaded, silver-decorated mesoporous silica nanoparticles. International Journal of Nanomedicine. 2017;Volume 12:3577-89. doi:https://doi.org/10.2147/ijn.s133846.

[16] Bobbarala V. Antimicrobial agents. ISBN 978-953-51-0723-1; 2021. doi:http://dx.doi.org/10.5772/1867.

[17] Lu Y, Yin Y, Li ZY, Xia Y. Synthesis and Self-Assembly of AuSiO2 Core-Shell Colloids. Nano Letters. 2002;2(7):785-8. doi:https://doi.org/10.1021/nl025598i.

[18] Jagtap S, Chopade P, Tadepalli S, Bhalerao A, Gosavi S. A review on the progress of ZnSe as inorganic scintillator. Opto-Electronics Review. 2019;27:90-103. doi:https://doi.org/10.1016/j.opelre.2019.01.001.

[19] Liu XH, Luo XH, Lu SX, Zhang JC, Cao WL. A novel cetyltrimethyl ammonium silver bromide complex and silver bromide nanoparticles obtained by the surfactant counterion. Journal of colloid and interface science. 2007;307:94-100. doi:https://doi.org/10.1016/j.jcis.2006.11.051.

[20] Sui Z, Chen X, Wang L, Chai Y, Yang C, Zhao J. An Improved Approach for Synthesis of Positively Charged Silver Nanoparticles. Chemistry Letters. 2005;34:100-1. doi:http://dx.doi.org/10.1246/cl.2005.100.

[21] Quan G, Pan X, Wang Z, Wu Q, Li G, Dian L, et al. Lactosaminated mesoporous silica nanoparticles for asialoglycoprotein receptor targeted anticancer drug delivery. Journal of Nanobiotechnology. 2015;13(1):7. doi:https://doi.org/10.1186/s12951-015-0068-6.

[22] Tan Z, Tan F, Zhao L, Li J. The Synthesis, Characterization and Application of Ciprofloxacin Complexes and Its Coordination with Copper, Manganese and Zirconium Ions. Journal of Crystallization Process and Technology. 2012;02:55-63. doi:http://dx.doi.org/10.4236/jcpt.2012.22008.

[23] Abd El-Zahir MS, Saleh SM, ElKady HA, Orabi AS. Ciprofloxacin Metal Complexes–Silica

Nanoparticles: Characterization, Spectroscopic Study, DNA Interaction and Biological Activity. Journal of Solution Chemistry. 2024;53:1269-93. doi:https://doi.org/10.1007/s10953-024-01375-7.

[24] Sahoo S, Chakraborti C, Naik S, Mishra S, Nanda U. Structural Analysis of Ciprofloxacin-Carbopol Polymeric Composites by X-Ray Diffraction and Fourier Transform Infra-Red Spectroscopy. Tropical Journal of Pharmaceutical Research. 2011;10. doi:https://doi.org/10.4314/tjpr.v10i3.14.

[25] Pandey S, Pandey P, Tiwari G, Tiwari R, Rai A. FTIR spectroscopy: A tool for quantitative analysis of ciprofloxacin in tablets. Indian Journal of Pharmaceutical Sciences. 2012;74(1):86. doi:https://doi.org/10.4103/0250-474X.102551.

[26] Niu J, Tang G, Tang J, Yang J, Zhou Z, Gao Y, et al. Functionalized Silver Nanocapsules with Improved Antibacterial Activity Using Silica Shells Modified with Quaternary Ammonium Polyethyleneimine as a Bacterial Cell-Targeting Agent. Journal of Agricultural and Food Chemistry. 2021;69:6485-94. doi:https://doi.org/10.1021/acs.jafc.1c01930.

[27] Ibraheem DR, Hussein NN, Sulaiman GM, Mohammed HA, Khan RA, Al Rugaie O. Ciprofloxacin-Loaded Silver Nanoparticles as Potent Nano-Antibiotics against Resistant Pathogenic Bacteria. Nanomaterials. 2022;12:2808. doi:https://doi.org/10.3390/nano12162808.